The Use of an Error Index to Improve Numerical Solutions for Unsteady Lifting Airfoils

Shigenori Ando* and Akio Ichikawa†
Nagoya University, Nagoya, Japan

The numerical methods of the aerodynamic finite element method are investigated for airfoils in incompressible inviscid flow, using an "error index parameter." This method can compare large amounts of data in an efficient and precise manner. The first problem is a concentration of error at the airfoil edges, which occurs in all of the cases investigated. This difficulty can be solved by using the semicircular method of computation. The second problem results from the logarithmic singularity of the unsteady kernel function; the difficulty dramatically reduced through a special method for treating the logarithmic singularity. It is found that using the error index parameter has advantages for several schemes of quantizing lift distribution.

Nomenclature

b	= airfoil semichord = 1
CP	= control (or upwash) point or its location as fractions of the local element chord
E	= error index
EP	= error evaluation point or its location as fractions of the local element chord
h_ν	= length of domain for which the discretized lift is designated as $\bar{P}_\nu$
i	$=\sqrt{-1}$
i,j,ℓ,n,ν	= integers
k	= reduced frequency ω/U (since $b=1$)
K	= kernel function
K_{ij}	= matrix element resulting from discretizing kernel function
m	= integer for mth upwash mode ($w=-\cos m\theta$)
N	= total number of the lattices (elements)
Δp	= lift distribution, positive upward
P	$=\Delta p/\rho U^2$
U	= freestream velocity
w	= upwash velocity, positive upward
x	= chordwise coordinate (in most cases, of upwash points) $=-\cos\theta$
ρ	= air mass density
γ	= vortex density normalized by U or Euler's constant
Γ_{a_j}	= vortex strength nondimensionalized by $Ub=\gamma_{a_j}h_j$
ξ	= chordwise coordinate (in most cases, of loading points) $=-\cos\varphi$
ω	= angular frequency for simple harmonic variation in time

Subscripts and Superscripts

a	= approximate numerical value
e	= exact analytical value
$\bar{\ }$	= complex amplitude for simple harmonic variation in time
$(R),(I)$	= real and imaginary parts

Received April 29, 1981; revision received May 13, 1982.

*Professor, Department of Aeronautical Engineering. Member AIAA.

†Research Associate, Department of Aeronautical Engineering. Member AIAA.

I. Introduction

THIS paper discusses the numerical methods used to investigate unsteady lifting surfaces, with special attention given to airfoils in a two-dimensional incompressible inviscid flow. Many papers have been published in this field, but systematic comparative studies of their accuracy are few. This situation makes it difficult for aerodynamic engineers to select the most efficient method of numerical analysis for a particular problem.

Our concern here is the aerodynamic finite element method (AFEM) which includes lattice methods because some authors claim that these methods do not require any special approaches, even for somewhat irregular wing planforms and/or upwash distributions.[1] However, we find several points that can be improved.

It is evident that what is needed is an efficient way to answer the question: which of various numerical methods is the most efficient? For this purpose we introduce an "error index." This index is easily obtainable and often presents much more information than more elaborate analytical theorems of error, such as given by James.[2]

Section II describes comparative studies of three schemes which discretize the lift distribution of steady airfoils. In Sec. III it is found that the ordinary doublet lattice method (DLM) becomes inefficient for high reduced frequencies in the unsteady case, as suggested in Ref. 3. It is discovered that a special method for treating the logarithmic singularity in the kernel function improves this inefficiency dramatically.

II. Steady Incompressible Case

Scope

Most current methods for unsteady lifting airfoils utilize the integral equation (Ref. 4, p. 324),

$$\bar{w}(x)=\int_{-1}^{1}\bar{P}(\xi)K(x,\xi,k,M)\,\mathrm{d}\xi \tag{1}$$

where the kernel function K is singular at $\xi=x$. The semichord length is assumed to be unity. When the reduced frequency $k=0$ and the stream Mach number $M=0$, Eq. (1) reduces to (Ref. 4, p. 215)

$$w(x)=-\frac{1}{2\pi}\oint_{-1}^{1}\frac{\gamma(\xi)}{x-\xi}\,\mathrm{d}\xi \tag{2}$$

which includes the so-called Cauchy kernel. As shown later the Cauchy kernel appears to be essential even for the case of $k\neq 0$. Thus, it is useful to investigate the simplest integral

equation (2) first. Usual AFEMs discretize Eq. (2) as

$$w_i = \sum_{j=1}^{N} K_{ij} P_j \tag{3}$$

which is a set of simultaneous algebraic equations to be solved for P_j.

This section is limited to three schemes for discretizing lift distributions (see Fig. 1): δ,‡ step, and linear. In all of these schemes the full chord length is divided into equal segments. We also restrict the upwash distributions to $w = -\cos m\theta$, where $x = -\cos\theta$ and $m = 0,1,2,\ldots$.

James[2] published an elaborate analytical investigation of a similar subject, restricting himself primarily to a δ-type scheme with a zeroth upwash mode ($m = 0$). It should be noted that our approach using the "error index" is much easier than James' analytical one and that our investigation covers the three schemes in Fig. 1 with various upwash distributions of $m \geq 0$.

Exact Solutions

Using the Söhngen's inversion formula (Ref. 4, p. 217) of Eq. (2) for $w = -\cos m\theta$, we have

$$\begin{aligned} \gamma_e &= 2\sqrt{(1-\xi)/(1+\xi)}, & m &= 0 \\ &= -2\sin m\varphi, & m &\geq 1 \end{aligned} \tag{4}$$

Expressions for K_{ij}

Explicit expressions for K_{ij} in the three schemes are easily obtained by elementary methods. See Appendix B.

Error Evaluation Method

Introduction of Error Index

In the literature, comparisons among various methods are usually made using the lift coefficient, pitching moment coefficient, location of center of pressure, etc. Otherwise the lift distribution itself is used. Here, we introduce a single index which summarizes the errors in lift distribution,

$$E = \left[\sum_{\nu=1}^{N} |P_a - P_e|_\nu h_\nu\right] \Big/ \left[\sum_{\nu=1}^{N} |P_e|_\nu h_\nu\right], \quad h_\nu \equiv 2/N \tag{5}$$

P may be replaced by γ.

It has been confirmed through numerical experiments that this definition leads us to reasonable results. As shown later, the introduction of the error index enables us to compare large amounts of data in an efficient and precise manner.

Points for Error Evaluation

For the δ scheme, we locate the points for error evaluation at the quarter-chord point of each element. Specifically, an approximate value $\gamma_a(\xi_\nu)$ is compared with the exact value $\gamma_e(\xi_\nu)$. ξ_ν is the quarter-chord point of the νth element.

For the step-type scheme, the points for error evaluation are selected naturally at the center of each element. For the linear type, they are selected at both ends of each element except for $x = +1$, where $\gamma_a = \gamma_e = 0$ due to the Kutta condition.

Discussion of Results

Best Control Points

For δ distribution, the currently used control point (CP) at 75% chord of each element is best, except at $m = 0$ (see Fig. 2). There is no stable (unique) location of the optimum CP for

‡The term δ is used because of its resemblance to Dirac's delta function. See Appendix A.

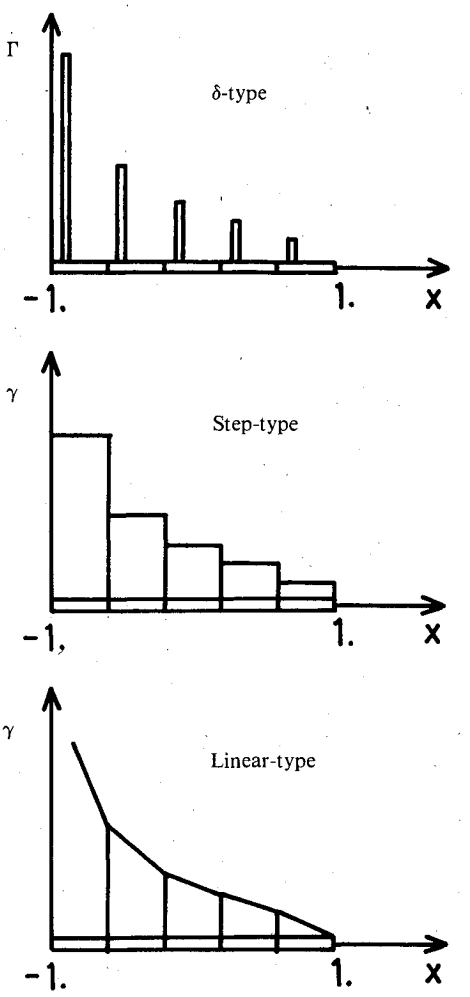

Fig. 1 Three schemes for discretizing lift distribution.

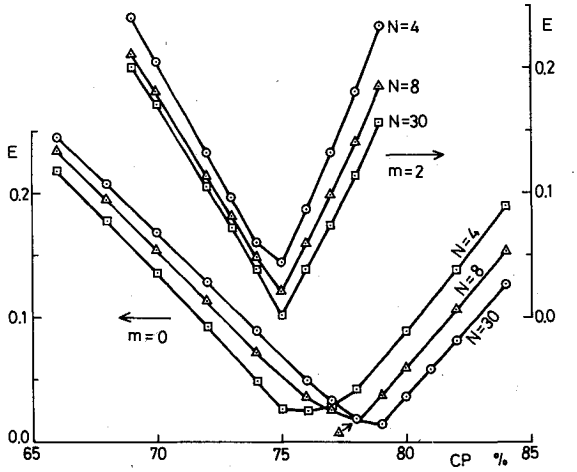

Fig. 2 Error index (E) vs control point (CP) for δ type.

$m = 0$, in that this E vs N curve is worse than those for $m \neq 0$. The step-type scheme has the best CP at 85-95%, but the exact best CP has not been defined uniquely. Accordingly, different investigators have selected a variety of CP positions[2,5,6] when using this scheme (see Fig. 3). James[2] has stated that CP = 50% is the poorest choice for this scheme which is doubtless because $|\det(K_{ij})|$ becomes minimum (zero for odd N). On the other hand, CP = 100% for this scheme makes the diagonal elements infinite when γ_a becomes indeterminate. These facts suggest why CP = 50 and 100% are unsuitable for the step-type discretizing scheme. For the

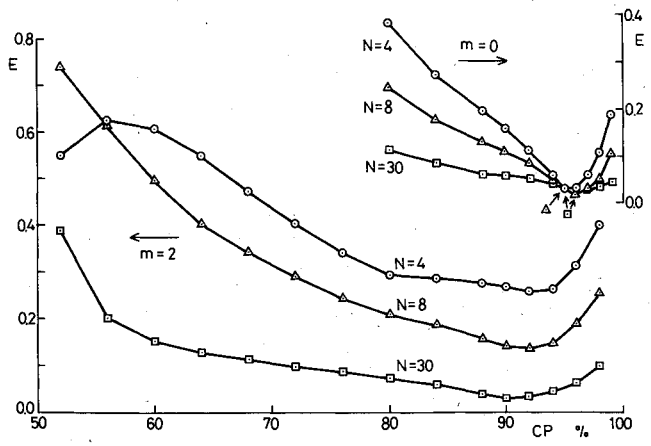

Fig. 3 Error index (E) vs control point (CP) for step type.

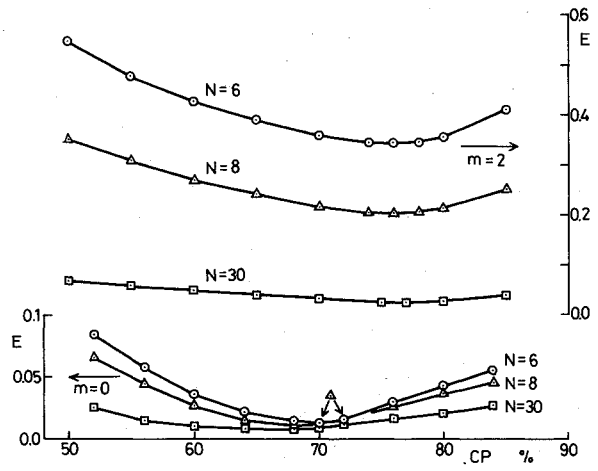

Fig. 4 Error index (E) vs control point (CP) for linear type.

linear-type scheme, the best CP location is more obscure, as seen from Fig. 4, where the E vs CP curves depict shallow bottoms at 65-80%.

Accuracy

Figure 5 shows E vs N plots for the δ-type scheme, where the solid curves refer to the equispaced division (ESD) and the dotted curves are obtained by the semicircular division (SCD), which is designated as "DLM-B." The details of the latter will be described below. It is found that E for $m=0$ is especially poor for ESD but less so for SCD, as has been pointed out by Lan.[6] Our method using the error index shows this even more distinctly than Lan did. This difference between the ESD and SCD results from the error concentration at the edges, as will be discussed later. Although the concentration ratio is the same for all m, the lift itself on the head element for $m=0$ in ESD is much larger than for $m\geq 1$ in ESD or for all m in SCD.

Figure 6 compares the δ-type (dashed lines) and the step-type (solid lines) schemes. It can be seen that the former is generally better than the latter. Figure 7 compares the δ (dashed) and the linear (solid) types. Here also the δ scheme is superior except at $m=0$. Note that the linearity of the E vs N curves is achieved most rapidly for the δ scheme as N increases. We generally find that the better method makes the E vs N curves linear more rapidly as N increases.

Concentration of Error

James[2] shows theoretically that the error concentrates at the head element at a rate of 11.4% for $m=0$ in the δ scheme. Our numerical research demonstrates this even for $m\geq 1$ in the δ-type approach (see Figs. 8 and 9). Similar results occur for step and linear schemes as well (see Fig. 8).

Satisfaction of the Kutta Condition

James[2] investigates theoretically how the numerical results satisfy the Kutta condition automatically for the δ scheme with $m=0$. This is recognized from our numerical experiments for both of the δ and step types for all $m\geq 0$. (This condition can be imposed before computations only for the linear-type scheme.)

III. Unsteady Incompressible Case

Scope

In the previous section we treated the steady case with the ESD (equispaced division) method. Here the unsteady case is studied with the SCD (semicircular division) method for the δ scheme, which has been recognized as the best in the steady case. The reason SCD is used rather than ESD is that SCD can alleviate the adverse effects of the error concentration at the head element, especially for $m=0$. The error index will also be

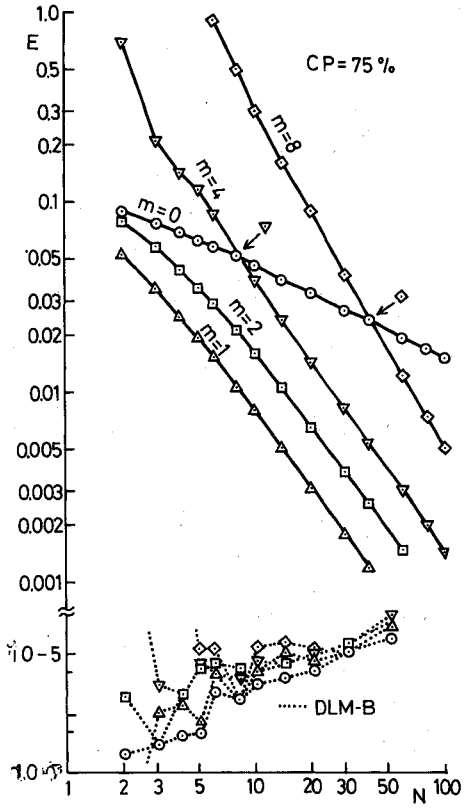

Fig. 5 E vs number of divisions (N) for δ type.

used here. The fundamental formulas for DLM are derived using Possio's integral equation (Ref. 4, p. 324), the exact solution to which is given by Schwarz (Ref. 4, p. 277).

Possio's Integral Equation

Possio's integral equation for unsteady airfoils in an incompressible flow is

$$\bar{w}(x) = -\frac{1}{2\pi}\int_{-1}^{1} \bar{P}(\xi)K(x,\xi,k)\,d\xi \tag{6}$$

where the kernel is given by

$$K = \frac{1}{x-\xi} - ike^{-is}[C_i(|s|) + i(S_i(s)+\pi/2)]$$

$$s \equiv k(x-\xi) \tag{7}$$

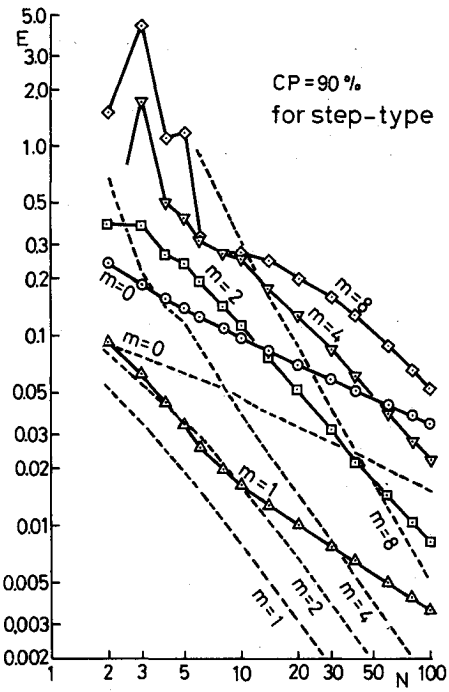

Fig. 6 *E* vs *N*, comparison between step type (solid lines) and δ type (dashed lines).

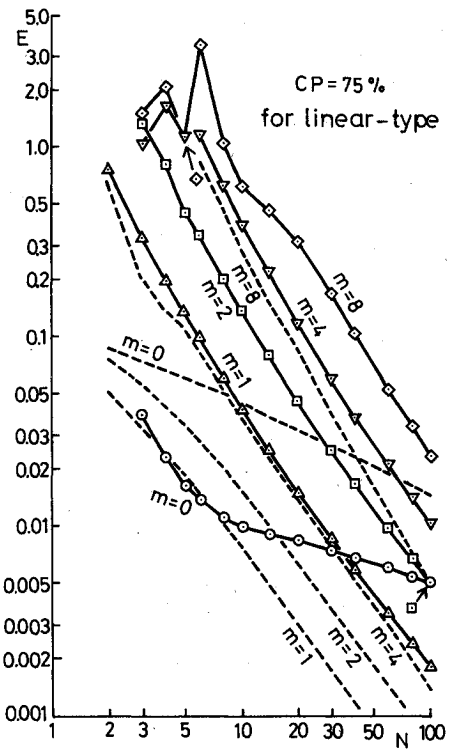

Fig. 7 *E* vs *N*, comparison between linear type (solid lines) and δ type (dashed lines).

S_i and C_i are the sine and cosine integrals, respectively. It is noteworthy that the argument of the C_i function must be the absolute value. This fact is pointed out without any proof in Ref. 7. We prove[8] this by recovering nonzero z (the coordinate normal to x) and making z vanish at an appropriate time.

Formulations of DLMs

DLM-A Method

This is a straightforward doublet-lattice method in which ESD is used.

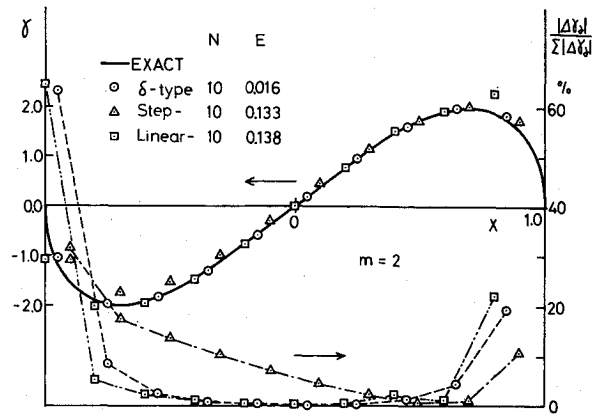

Fig. 8 Distribution of error for δ, step, and linear types ($m=2$).

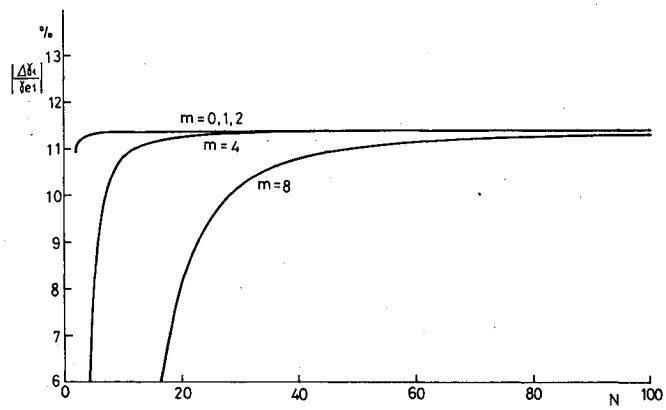

Fig. 9 Concentration ratio of error at the head element for δ type.

DLM-B Method

The formulation of this scheme is given as

$$\bar{w}(\theta_\ell) = -1/(2N+1) \sum_{j=1}^{N} K_{\ell j} \bar{P}_j \tag{8}$$

$$K_{\ell j} = \frac{\sin\varphi_j}{\cos\varphi_j - \cos\theta_\ell} - ike^{-is}[C_i(|s|) + i(S_i(s) + \pi/2)]\sin\varphi_j$$

$$s = k(\cos\varphi_j - \cos\theta_\ell), \quad \bar{P}_j = \bar{P}(\varphi_j)$$

$$\varphi_j = (2j-1)\pi/(2N+1), \quad \theta_\ell = 2\ell\pi/(2N+1)$$

$$\ell, j = 1,2,3,\ldots N \tag{9}$$

To obtain the above formulation, the following are used

$$\int_{-1}^{1} \sqrt{\frac{1-\xi}{1+\xi}} f(\xi)\,d\xi = \frac{2\pi}{2N+1} \sum_{j=1}^{N} (1-\xi_j) f_j + 0(f^{(2N)}) \tag{10}$$

$$\int_{-1}^{1} \sqrt{\frac{1-\xi}{1+\xi}} \frac{f(\xi)}{x_\ell - \xi}\,d\xi = \frac{2\pi}{2N+1} \sum_{j=1}^{N} \frac{1-\xi_j}{x_\ell - \xi_j} f_j + 0(f^{(2N+1)}) \tag{11}$$

$$x_\ell = -\cos\theta_\ell, \qquad \xi_i = -\cos\varphi_j \tag{12}$$

Equation (10) is the well-known Gauss' quadrature and Eq. (11) is Stark's formula[9] applied with the special weighting function $\sqrt{(1-\xi)/(1+\xi)}$. Equation (10) is used for all terms, except the Cauchy kernel to which Eq. (11) is applied. A logarithmic singularity term in the kernel is treated as if it were regular.

DLM-C Method

The kernel of Eq. (7) includes a logarithmic singularity, since

$$C_i(|s|)=[\gamma+\ell nk+C_i^*(|s|)]+\ell n|x-\xi| \tag{13}$$

where γ is the Euler's constant 0.57721 and

$$C_i^*(s)\equiv\int_0^s(\cos t-1)t^{-1}\mathrm{d}t \tag{14}$$

Here $C_i^*(s)$ is regular. It is found that both DLM-A and -B yield poor numerical results as k increases. Hence the DLM-C contains a special device to treat the logarithmic singularity. Substituting Eqs. (7) and (13) into Eq. (6), we have

$$\bar{w}(x)=-\frac{1}{2\pi}[I_R-ike^{-ikx}I_{\log}] \tag{15}$$

where

$$I_{\log}\equiv\int_{-1}^{1}e^{ik\xi}\ell n|x-\xi|\bar{P}(\xi)\mathrm{d}\xi \tag{16}$$

I_R results from the remaining parts of the kernel. $\bar{P}(\xi)$ may be written as

$$\bar{P}(\xi)e^{ik\xi}\equiv\sqrt{(1-\xi)/(1+\xi)}f(\xi) \tag{17}$$

where $f(\xi)$ is a well-behaved function. Using Eq. (17) and putting $x=-\cos\theta$ and $\xi=-\cos\varphi$ in Eq. (16) yields

$$I_{\log}=\int_0^{\pi}(1+\cos\varphi)\ell n|\cos\theta-\cos\varphi|f(\varphi)\mathrm{d}\varphi \tag{18}$$

where $f(-\cos\varphi)$ is written as $f(\varphi)$ for simplicity. Now let us use the interpolated expression of $f(\varphi)$

$$f(\varphi)=\sum_{j=1}^{N}g_j(\varphi)f_j,\quad f_j\equiv f(\varphi_j) \tag{19}$$

where $g_j(\varphi)$ is the interpolation function based on the weighting function $\sqrt{(1-\xi)/(1+\xi)}$

$$g_j(\varphi)=\frac{4}{2N+1}\frac{\cos\varphi_i/2}{\cos\varphi/2}\sum_{n=0}^{N-1}\cos(2n+1)\frac{\varphi_i}{2}\cos(2n+1)\frac{\varphi}{2}$$

$$\varphi_j=(2j-1)\pi/(2N+1),\quad j=1,2,\ldots N \tag{20}$$

See, for example, Ref. 10. Substitution of Eqs. (19) and (20) into Eq. (18) requires evaluation of the integral

$$\hat{I}_n=\frac{1}{\pi}\int_0^{\pi}\cos n\varphi\ell n|\cos\theta-\cos\varphi|\mathrm{d}\varphi \tag{21a}$$

$$\hat{I}_n=-\ell n2,\qquad \text{for } n=0$$

$$=-(1/n)\cos n\theta,\qquad \text{for } n\geq 1 \tag{21b}$$

which is obtained by using the formula

$$\ell n|\cos\theta-\cos\varphi|=-\ell n2-2\sum_{r=0}^{\infty}\frac{1}{r}\cos r\theta\cos r\varphi \tag{22}$$

Thus we have

$$I_{\log}(\theta)=\sum_{j=1}^{N}A_j(\theta)f_j$$

$$A_j(\theta)=\frac{4}{2N+1}\cos\frac{\varphi_j}{2}\sum_{n=0}^{N-1}\cos(2n+1)\frac{\varphi_j}{2}F_n(\theta)$$

$$F_n(\theta)=-\pi(\cos\theta+\ell n2),\qquad n=0$$

$$=-\pi\left(\frac{\cos n\theta}{n}+\frac{\cos(n+1)\theta}{n+1}\right),\qquad n\geq 1 \tag{23}$$

Now we must restore $\bar{P}$ from f, using

$$f_j=e^{ik\xi_j}\bar{P}_j\tan\varphi_j/2 \tag{24}$$

The remaining parts of Eq. (15), I_R, are treated by using Eqs. (10-12) just as in the DLM-B. Then we arrive at the following formulation of DLM-C

$$\bar{w}(\theta_\ell)=-\frac{1}{2N+1}\sum_{j=1}^{N}K_{\ell j}\bar{P}_j$$

where

$$K_{\ell j}\equiv\frac{\sin\varphi_j}{\cos\varphi_j-\cos\theta_\ell}-ike^{-is}[R(s)+L_{\ell j}]\sin\varphi_j$$

$$R(s)=C_i^*(|s|)+i[S_i(s)+\pi/2]+\gamma+\ell nk$$

$$L_{\ell j}\equiv\frac{1}{\pi}\sum_{n=0}^{N-1}\left[\cos n\varphi_j-\sin n\varphi_j\tan\frac{\varphi_j}{2}\right]F_n(\theta_\ell) \tag{25}$$

The only difference between DLM-B and -C lies in the treatment of the $I_{\log}$ term. In the former it is discretized through Eq. (10), assuming that the logarithmic kernel may be included in $f(\xi)$.

Error Evaluation Method

As in Sec. II, we introduced an error index which should be slightly modified as follows,

$$E\equiv(E^{(R)}+E^{(I)})/2$$

$$E^{(R),(I)}\equiv\left[\sum_{\nu=1}^{N}|\bar{P}_a-\bar{P}_e|_\nu^{(R),(I)}h_\nu\right]\Big/\left[\sum_{\nu=1}^{N}|P_e^{(R),(I)}|_\nu h_\nu\right]$$

$$h_\nu\equiv(\pi/N)\sin\theta_\nu,\quad \theta_\nu\equiv(2\nu-1)\pi/(2N-1)$$

$$\nu=1,2,\ldots N \tag{26}$$

It is recognized again that E defined in such a manner leads us to results compatible with various intuitive feelings.

Discussion of Results

Figure 10 compares the lift distributions obtained by the DLM-A and -C methods and the Schwarz' exact solution for $\bar{w}=-1$, $k=5$, and $N=10$. The superiority of the DLM-C is surprising. Another comparison of the E vs N plots of DLM-A and -C is presented in Fig. 11 for $\bar{w}=-1$ and various k. Large decreases in E for DLM-C occur as N increases, whereas this is not so for DLM-A. The plots for DLM-C (dotted lines) result from the accuracy limits of the single precision method. An additional comparison of the E vs k plots is given in Fig. 12, which shows that DLM-B also deteriorates for nonzero k. Thus SCD itself cannot improve nonsteady accuracy. However, the effect of SCD is dramatic for the steady case, as seen in Fig. 13, which suggests that the edge concentration of the error is the only important problem

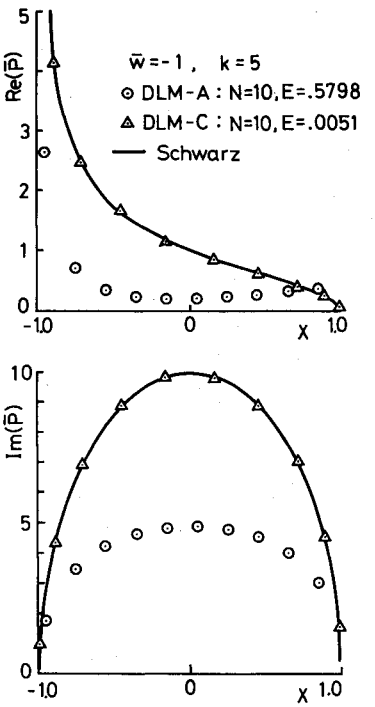

Fig. 10 Distribution of lift, comparison between DLM-A, DLM-C, and Schwarz' exact solution.

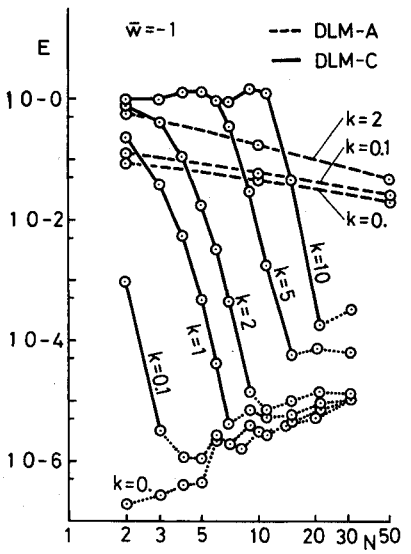

Fig. 11 E vs N, comparison between DLM-A and -C for various reduced frequencies k.

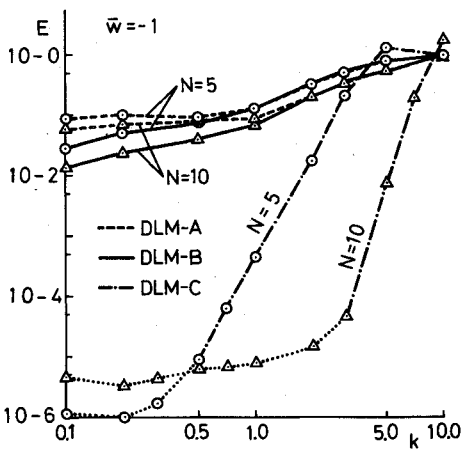

Fig. 12 E vs k comparison between DLM-A, -B, and -C for various numbers of division N.

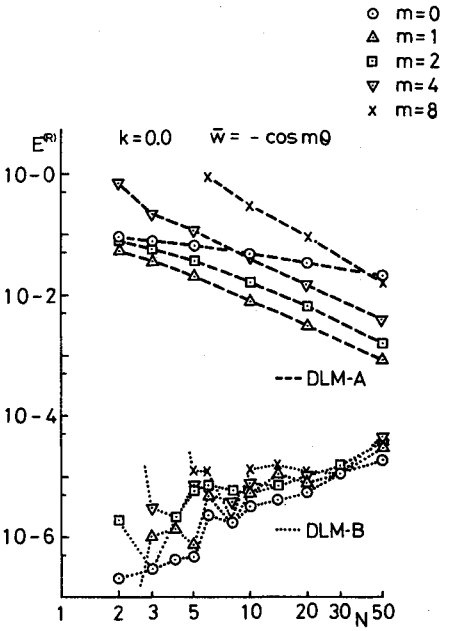

Fig. 13 $E^{(R)}$ vs N, comparison between DLM-A and -B for various upwash modes m.

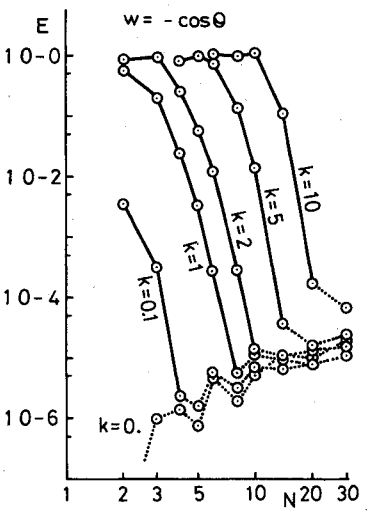

Fig. 14 E vs N for DLM-C, $m=1$ and various reduced frequencies k.

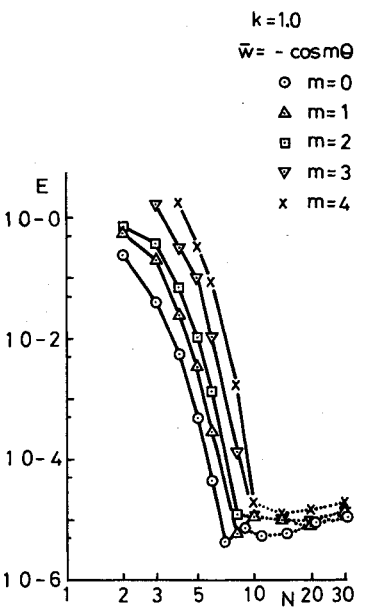

Fig. 15 E vs N for DLM-C, $k=1$ and various upwash modes m.

for the steady case. Incidentally, we confirmed that an alternative SCD scheme developed by Lan[6]

$$\xi_k = -\cos(2k-1)\pi/2N, \quad x_i = -\cos i\pi/N, \quad k,i=1,2,3,\ldots N \tag{27}$$

gives nearly the same numerical results. Figure 14 shows E vs N plots for $m=1$ and various k, which is obtained using DLM-C. It is seen that increasing k from 1 to 10 requires about a threefold increase in N. Figure 15 shows a similar diagram for $k=1$ and various m. We recognize that increasing m by 1 requires increasing N by only about 1 when the DLM-C method is adopted.

It is evident from all of these illustrations that if the DLM-C method is used increases in m and k cause no essential difficulties.

IV. Conclusions

Numerical methods belonging to the AFEM (aerodynamic finite element method) are discussed for airfoils in incompressible inviscid flow, using an error index parameter. The index provides a method for comparing large amounts of data in a compact and precise manner. The upwash distributions are restricted to the types of $\bar{w}=-\cos m\theta$, $m=0,1,2,\ldots$. The δ type of discretization is superior to the step and linear types. Concentration of the error at the edge elements (especially the leading edge) is recognized for all cases investigated. This occurs most severely for the case of $\bar{w}=\text{const}$ ($m=0$) when the ESD (equispaced division) scheme is used. Adoption of the SCD (semicircular division) method solves this difficulty completely. Unsteadiness adds another problem that results from the logarithmic singularity of the kernel. Expansion of this term into the Fourier series and the use of an interpolation function lead us to a method which yields significant improvement. It is noteworthy that the error index introduced here plays an important role in all of the methods used.

Appendix A: General Formulation of DLMs

Consider

$$\bar{w}(x) = \int_{-1}^{1} \bar{P}(\xi) K(x-\xi)\,\mathrm{d}\xi \tag{A1}$$

There are two general formulations of DLMs from Eq. (A1).

Formulation 1

The unknown $\bar{P}(\xi)$ is written as

$$\bar{P}(\xi) = \sum_{\nu=1}^{N} \bar{P}_\nu \delta(\xi-\xi_\nu) h_\nu \tag{A2}$$

where δ is the Dirac delta function. Substituting Eq. (A2) into Eq. (A1), we have

$$\bar{w}(x) = \sum_{\nu=1}^{N} \bar{P}_\nu K(x-\xi_\nu) h_\nu \tag{A3}$$

This scheme may be a primitive version of DLM, which is used for ESD in the text.

Formulation 2

The right-hand side of Eq. (A1) may be divided into three basic forms

$$\int_{-1}^{1} \sqrt{\frac{1-\xi}{1+\xi}} f(\xi) K_i(x-\xi)\,\mathrm{d}\xi, \quad i=1,2,3 \tag{A4}$$

where K_1 is regular, $K_2=1/(x-\xi)$, and $K_3=\ell n|x-\xi|$. Use of the interpolation function based on the weighting function $\sqrt{(1-\xi)/(1+\xi)}$ leads us to DLMs with SCD. DLM-B and -C in the text are the examples.

Appendix B: K_{ij} for the Steady Case

Let us define K_{ij} with the following equation,

$$w_i = -\frac{1}{2\pi} \sum_{j=1}^{N} K_{ij} \gamma_{a_j} \tag{B1}$$

Then for the δ type,

$$K_{ij} = 1/[i-j+(\mathrm{CP}-0.25)] \tag{B2}$$

for the step type,

$$K_{ij} = \ell n \left| \frac{i-j+\mathrm{CP}}{i-j-1+\mathrm{CP}} \right| \tag{B3}$$

and for the linear type;

when $m \geq 1$

$$K_{i1} = 1-(i-2+\mathrm{CP})\ell n \left| \frac{i-1+\mathrm{CP}}{i-2+\mathrm{CP}} \right|$$

$$K_{ij} = (i-j+1+\mathrm{CP})\ell n \left| \frac{i-j+1+\mathrm{CP}}{i-j+\mathrm{CP}} \right|$$

$$-(i-j-1+\mathrm{CP})\ell n \left| \frac{i-j+\mathrm{CP}}{i-j-1+\mathrm{CP}} \right| \qquad j \geq 2 \tag{B4}$$

When $m=0$, we assume that γ_a in the head element takes the form of $C'\sqrt{(1-\xi)/(1+\xi)}$. The constant C' is an unknown and must be determined by using the fact that the γ_a passes the front end of the second element. Thus we have

$$K_{i2} = \frac{1}{\sqrt{N-1}} \left(\pi - 2\tan^{-1}\sqrt{N-1} - Q\ell n \left| \frac{\sqrt{N-1}-Q}{\sqrt{N-1}+Q} \right| \right)$$

$$+1-(i-3+\mathrm{CP})\ell n \left| \frac{i-2+\mathrm{CP}}{i-3+\mathrm{CP}} \right|, \quad Q \equiv \sqrt{\frac{N-i+1-\mathrm{CP}}{i-1+\mathrm{CP}}}$$

$$K_{ij} = (i-j+1+\mathrm{CP})\ell n \left| \frac{i-j+1+\mathrm{CP}}{i-j+\mathrm{CP}} \right|$$

$$-(i-j-1+\mathrm{CP})\ell n \left| \frac{i-j+\mathrm{CP}}{i-j-1+\mathrm{CP}} \right| \qquad j \geq 3 \tag{B5}$$

Acknowledgment

The authors wish to thank Professors I. Tani and K. Tamada and Dr. C. F. Hansen for their valuable criticism and guidance.

References

[1] Albano, E. and Rodden, W. P., "A Doublet Lattice Method for Calculating Lift Distribution on Oscillating Surfaces in Subsonic Flows," *AIAA Journal*, Vol. 7, Feb. 1969, pp. 279-285.

[2] James, R.M., "On the Remarkable Accuracy of the Vortex Lattice Method," *Computer Methods in Applied Mechanics and Engineering*, Vol. 1, 1972, pp. 59-79.

[3] Landahl, M. T. and Stark, V.J.E., "Numerical Lifting-Surface Theory—Problems and Progress," *AIAA Journal*, Vol. 6, Nov. 1968, pp. 2049-2060.

[4] Bisplinghoff, R. L. et al., *Aeroelasticity*, Addison-Wesley, Reading, Mass., 1959.

[5] Woodward, F. A., "Analysis and Design of Wing-Body Combinations at Subsonic and Supersonic Speeds," *Journal of Aircraft*, Vol. 5, June 1968, pp. 528-534.

[6] Lan, C. E., "A Quasi-Vortex-Lattice Method in Thin Wing Theory," *Journal of Aircraft*, Vol. 11, Sept. 1974, pp. 518-527.

[7] Fromme, J. and Goldberg, M., "Unsteady Two-Dimensional Airloads Acting on Oscillating Thin Airfoils in Subsonic Ventilated Wind Tunnels," NASA CR 2967, 1978.

[8] Ichikawa, A. and Ando, S, "Accuracy of Numerical Method for Unsteady Subsonic Lifting Airfoils," *Journal of Japan Society for Aerospace Sciences*, Vol. 29, No. 325, 1980, pp. 11-18 (in Japanese).

[9] Stark, V.J.E., "A Generalized Quadrature Formula for Cauchy Integrals," *AIAA Journal*, Vol. 9, Sept. 1971, pp. 1854-1855.

[10] Davies, D. E., "Calculation of Unsteady Generalized Air Forces on a Thin Wing Oscillating Harmonically in Subsonic Flow," British R&M 3409, 1965.